# PCCP

Accepted Manuscript

This article can be cited before page numbers have been issued, to do this please use: W. Jiang, Y. Qiang, M. Liu, W. Li, F. Qiu and A. Shi, *Phys. Chem. Chem. Phys.*, 2017, DOI: 10.1039/C7CP03718J.




ROYAL SOCIETY OF CHEMISTRY

rsc.li/pccp

View Article Online
DOI: 10.1039/C7CP03718J





# Tetragonal phase of cylinders self-assembled from binary blends of AB diblock and $(A'B)_n$ star copolymers

Wenbo Jiang,[a] Yicheng Qiang,[a] Meijiao Liu,[b] Weihua Li,*[a] Feng Qiu,[a] and An-Chang Shi[c]

The phase behavior of binary blends composed of AB diblock and $(A'B)_n$ star copolymers is studied using the polymeric self-consistent field theory, focusing on the formation and stability of stable tetragonal phase of cylinders. In general, cylindrical domains self-assembled from AB-type block copolymers are packed into a hexagonal array, although a tetragonal array of cylinders could be more favourable for lithography applications in microelectronics. The polymer blends are designed such that there is an attractive interaction between the A and A′ blocks, which increases the compatibility between the two copolymers and thus suppresses macroscopic phase separation of the blends. With a proper choice of system parameters, a considerable stability window for the targeted tetragonal phase is identified in the blends. Importantly, the transition mechanism between the hexagonal and tetragonal phases is elucidated by examining the distribution of the two types of copolymers in the unit cell of structure. The results reveal that the short $(A'B)_n$ star copolymers are preferentially located in the bonding area connecting two neighboring domains in order to reduce extra stretching, whereas the long AB diblock copolymers are extended to further space of the unit cell.

## 1 Introduction

Block copolymers have been regarded as a type of advanced materials due to its unique ability of self-assembly into diverse ordered nanostructures. The rich symmetries and the nanoscale feature size of these phases make them ideal candidates for potential applications in a wide range of fields.[1–6] For example, the gyroid phase of block copolymers has been considered as an ideal morphology for permeable membranes and polymeric solar cells because the unique gyroidal morphology provides bicontinuous channels for the transportation of small molecules[7] or charge carriers[6]. In contrast to the gyroid phase, the ordered phases (e.g. lamella, cylinder and sphere) have much simpler domain geometry. However these ordered phases still have the potential for applications in semiconductor industry via the fast advancing technique of directed self-assembly (DSA) that embeds the self-assembly of block copolymers on the length scale of sub-30nm into the traditional lithography technique.[8–10] The DSA of block copolymers has been successfully applied to fabricate large-scale defect-free stripes[8] and standing cylinders targeting at the applications of manufacturing quantum dot arrays for lasers[9] or high-density magnetic storage media.[10–12] The DSA of block copolymers has also been used to fabricate device-oriented irregular structures.[13–16] These advances have placed the DSA of block copolymers as one of the most promising next-generation bottom-up lithography techniques.[17–20]

For applications in semiconductor devices, a square cylindrical phase is more preferable than a hexagonal cylindrical phase because the square array is more compatible with the industry-standard coordinate system.[21] However, AB-type block copolymers with many topologies usually form the hexagonal phase.[22–24] Even imposing a strong external field in the form of lateral square confinement, it remains difficult to achieve a square pattern with cylinder-forming diblock copolymer.[25,26] A more effective approach is to devise new block copolymers that could self-assemble into a cylindrical phase with a tetragonal symmetry.[27]

It is well known that ABC linear triblock copolymers could form a cylindrical phase arranged on a square lattice where the A and C cylindrical domains are alternatively arranged on two sublattices.[28–31] However, the tetragonal cylinder phase of the AB-type block copolymers that is composed of one type of cylinders is significantly different from that formed in the ABC-type system, which is composed of two types of cylinders. Even within the constraint of two types of monomers, there exists a vast library

[a] State Key Laboratory of Molecular Engineering of Polymers, Collaborative Innovation Center of Polymers and Polymer Composite Materials, Department of Macromolecular Science, Fudan University, Shanghai 200433, China. E-mail:weihuali@fudan.edu.cn
[b] Department of Chemistry, Key Laboratory of Advanced Textile Materials and Manufacturing Technology of Education Ministry, Zhejiang Sci-Tech University, Hangzhou 310018, China
[c] Department of Physics and Astronomy, McMaster University, Hamilton, Ontario, Canada L8S 4M1

View Article Online
DOI: 10.1039/C7CP03718J





of chain architectures, providing the possibility to target at the desired AB-type block copolymers, but at the same time, also presenting a big challenge because simply searching the architecture space seems to be a formidable task.[32]

With the development of advanced synthetic techniques, more and more macromolecules with complex architectures can be precisely tailored, which provides a huge space for possible self-assembly structures.[32] It has been reported by experiments that square cylindrical phase could be formed from the self-assembly of copolymeric liquid crystal (LC) dendrimers[33] and dendronized polymer-liquid complexes.[34] Inspired by the experiments, Lee et al. performed a systematic study using self-consistent field theory (SCFT) on the self-assembly of the dendritic "pitchfork-like" block copolymers, and they concluded that the specific chain topology composed of a long handle and a moderate length of the dendron plays a crucial role on the formation of stable square cylindrical phase.[27] Based on these observations, recently Gao et al. further proposed an entropy-driven mechanism as an additional factor to the immiscibility and composition parameters that remarkably alters the self-assembly behavior of multi-arm block copolymers, e.g. regulating the packing lattice of cylindrical or spherical domains from classical to non-classical.[35] According to this mechanism, a $(BAB)_n$ star copolymer is purposely designed and a stability region of the desired square cylindrical phase is identified in the phase diagram of the bicomponent block copolymer.

Although $(BAB)_n$ star copolymers are accessible by modern synthetic techniques, they only exhibit a narrow stability region of the square cylindrical phase. It is therefore necessary to explore different block copolymer systems exhibiting a larger stability region of the square cylindrical phase. Besides providing alternative routes to engineering the same structure, studying the formation of the same structure from different block copolymer systems would provide a good understanding for the self-assembly mechanisms of desirable phases. Furthermore the availability of multiple block copolymer systems for the formation of the same ordered phase provides flexibility for the manufacturing of these structures. Besides tailoring the polymer architecture directly, blending different polymers offers an cost-effective route to regulate the self-assembly of block copolymers for novel structures. In particular, polymer blends could be used to enrich the phase behaviours of self-assembly polymers, e.g. adjusting the composition of block copolymers or domain spacing by adding the relevant homopolymers[36–38], or even targeting on new structures by blending different block copolymers, which cannot be formed in the pure constitutive copolymers.[39–42]

For polymer blends, there is always a tendency for the different polymers to phase separate. Macroscopic phase separation could be suppressed by introducing certain attractive interactions, e.g. hydrogen bonding, between the unlike polymers.[43–45] In experiments, hydrogen bonding has been widely used to combine different (co)polymers together to co-form an ordered microstructure. For example, Tang et al. blended AB [poly(ethylene oxide)-*b*-poly(styrene-r-4-hydroxystyrene), PEO-*b*-P(S-*r*-4HS)] and B′C [poly(styrene-*r*-4-vinylpyridine)-*b*-poly(methyl methacrylate), P(S-*r*-4VP)-*b*-PMMA] diblock copolymers, where B and B′ blocks have tuneable hydrogen bonding interactions, to form the A/C alternative tetragonal cylindrical phase.[46] Interestingly, the interaction parameter between A (or C) and B is same as that between A (or C) and B′. As a standard model system with hydrogen bonding interactions, this blend has been widely used for studying the effect of the hydrogen bonding interaction on the phase behaviors of the blend.[21,47]

In the current study, we focus on the design of a binary blend composed of the AB diblock copolymers and another relatively easy-accessed AB-type block copolymer in experiments,[48–50] aiming to generate stable square cylindrical phase. It has been revealed that the transition from the hexagonal phase to the square phase is driven by reducing the length of the effective bonds between neighboring domains that are constructed via bridging configurations in pure $(BAB)_n$ star copolymers.[35] In multi-arm block copolymers, the arms tend to be partitioned into neighboring as possible to maximize the configurational entropy. In other words, an overall spherical conformation is preferred by a multi-arm block copolymer. The entropy of partitioning the different arms in different domains is referred to as the combinatorial entropy. Importantly, the bridging configuration is strengthened by the large effect of the combinatorial entropy of the block copolymers with a large number of arms.[51,52]

To reduce the complexity of the copolymer architecture without loss of the critical factor forming effective bonds, we replace the $(BAB)_n$ triblock star copolymer with the simpler $(A'B)_n$ diblock star copolymer, and blend it with an AB diblock copolymer. One important alternation of the proposed copolymers is that the minority A and A′ blocks represent chains functionalized to act as donors and acceptors, respectively, such that the A and A′ blocks could possess attractive non-covalent (e.g. hydrogen) bonding interactions. It is important to note that the AB/$(A'B)_n$ blend is not a true AB-type system due to the presence of a negative interaction between the A and A′ blocks. However, the AB/$(A'B)_n$ blend could form ordered phases with one type of cylindrical domains composed of the A and A′ blocks. On the other hand, an ABC block copolymer system would form ordered phases with two types of cylindrical domains composed of A and C blocks, respectively. From this perspective, the AB/$(A'B)_n$ blending system is significantly different from the ABC system. Specifically, the AB diblock copolymer is intentionally chosen to be significantly longer than that of each arm of the star copolymer. We expect that the optimized distribution of the two copolymers with tailored controlling parameters will lead to the formation of the square cylindrical phase, where the shorter B blocks of $(A'B)_n$ are mainly distributed in the *bonding* area between two neighboring domains while the longer B blocks of AB are used to fill the central area of the square unit cell. More critically, the effective bond formed by the star copolymers could be regulated by varying the controlling parameters such as the length or the volume fraction of the $(A'B)_n$ star relative to the AB diblock, and thus it drives the transformation of the domain arrangement (or coordination number, CN).

It is important to note that the transformation of the domain arrangement is mainly dictated by the competition of the combinatorial entropy and the stretching energy. As long AB diblock

View Article Online
DOI: 10.1039/C7CP03718J





copolymers are added, the star copolymers in the hexagonal cylinders become more stretched and thus are forced to be in the bonding areas bridging two neighboring domains. If more AB diblock copolymers are added, the increasingly stretched bridging blocks would disrupt the effective bonds. One efficient way for the self-assembly system to delay this bond disruption is to form a new array of cylinders with fewer nearest-neighboring domains, i.e. the tetragonal phase whose smaller domain size and spacing is helpful to reduce the extra stretching of the effective bonds. When most of the bridge configurations are unavoidably disrupted in the tetragonal phase due to the extreme swelling of the AB diblocks, the tetragonal phase loses its advantage in the combinatorial entropy and would transform back into the hexagonal phase.

The stability of the targeted square phase is examined by comparing its free energy with other competing ordered phases in the interested parameter space. The free energy of each candidate phase is determined by the SCFT calculations. Although SCFT includes some approximations such as Gaussian-chain model and mean-field treatment, it has been proven to be one of the most successful methods on the study of phase behaviours of inhomogeneous polymers, especially producing a reliable accuracy with the determination of order-order transitions.[53,54] Considering possible macrophase separations, we proceed the SCFT calculations in the grand canonical ensemble,[36,55] and thus are able to determine the coexistence region of two neighboring phases.

## 2 Theory and method

We consider a binary blend consisting of AB diblock copolymers and an $(A'B)_n$ star copolymers in a given volume $V$. The star copolymer is composed of $n$ arms of A′B diblocks joined together at the ends of the B blocks (Figure 1). The two block copolymers are characterized by their chain length and block ratio of the A block, $N_i$ and $f_i$ ($i = 1$ for AB diblock and $i = 2$ for $(A'B)_n$ star copolymer). It is assumed that the three different blocks have equal Kuhn length $b$ and segment density $\rho_0$. For the convenience of modeling, we set $N_2 = n(N_{A',2} + N_{B,2}) = N$ as a reference length, and $\gamma = N_1/N_2$ denotes the length ratio of the AB diblock to the $(A'B)_n$ star. The generally repulsive interaction between the A (or A′) and B monomers is quantified by a Flory-Huggins parameter, $\chi_{AB} = \chi_{A'B}$, and the attractive interaction between the A and A′ monomers is quantified by a negative $\chi_{AA'}$.

The use of a negative interaction parameter to model hydrogen bonding needs to be justified. Dehghan and Shi showed that a general inter-polymer complexation model (ICM) provides a more accurate description of polymer blends with hydrogen bonding interactions.[43] In the same paper, Dehghan and Shi also concluded that the attractive-interaction model (AIM) provides a simple and fast method to obtain a qualitative understanding of the phase behavior of polymer blends with hydrogen bonding. Furthermore, they argued that the AIM could provide accurate phase behavior of blends of block copolymers with hydrogen bonding because the difference between the AIM and ICM diminishes when there is local phase separation of the different blocks. Based on these arguments, we decided to use a negative $\chi$ parameter for the hydrogen bonding interaction in the study of the phase behavior of the phase separated blend.[43,56]

In the grand-canonical ensemble, the chain numbers of AB diblock and $(A'B)_n$ star, $n_1$ and $n_2$ are regulated by their chemical potentials, $\mu_1$ and $\mu_2$, respectively. In practice, only one of the two chemical potentials is independent under the incompressibility condition. Without loss of generality, we choose the controlling parameter as $\mu_2$ while setting $\mu_1 = 0$. Within the Gaussian-chain model for all polymers, the free energy under the mean-field approximation in the unit of thermal energy $k_BT$, where $k_B$ is the Boltzmann constant and $T$ is temperature, can be expressed as,[36]

$$\begin{aligned}\frac{NF}{V\rho_0 k_B T} &= -Q_1 - z_2 Q_2 \\ &+\frac{1}{V}\int d\mathbf{r}\{\chi_{AB}N\phi_A(\mathbf{r})\phi_B(\mathbf{r}) + \chi_{A'B}N\phi_{A'}(\mathbf{r})\phi_B(\mathbf{r}) \\ &+\chi_{AA'}N\phi_A(\mathbf{r})\phi_{A'}(\mathbf{r}) - w_A(\mathbf{r})\phi_A(\mathbf{r}) - w_B(\mathbf{r})\phi_B(\mathbf{r}) - w_{A'}(\mathbf{r})\phi_{A'}(\mathbf{r}) \\ &-\eta(\mathbf{r})[1-\phi_A(\mathbf{r})-\phi_{A'}(\mathbf{r})-\phi_B(\mathbf{r})]\}, \end{aligned} \quad (1)$$

where $z_2 = \exp(\mu_2/k_BT)$ is the activity. $\phi_A(\mathbf{r})$ (or $\phi_{A'}(\mathbf{r})$) and $\phi_B(\mathbf{r})$ are the density functions of the A (or A′) and B monomers, and $w_A(\mathbf{r})$ (or $w_{A'}(\mathbf{r})$) and $w_B(\mathbf{r})$ are the correspondent density fields acting on A (or A′) and B monomers. The function $\eta(\mathbf{r})$ is a Lagrange multiplier enforcing the incompressibility condition, $\phi_A(\mathbf{r}) + \phi_{A'}(\mathbf{r}) + \phi_B(\mathbf{r}) = 1$. The two quantities $Q_1$ and $Q_2$ are the single chain partition functions[54] of the two copolymers interacting with the fields $w_A(\mathbf{r})$, $w_{A'}(\mathbf{r})$ and $w_B(\mathbf{r})$, which are given by,

$$Q_1 = \frac{1}{V}\int d\mathbf{r}\; q_1(\mathbf{r},s)q_1^\dagger(\mathbf{r},s), \quad (2)$$

$$Q_2 = \frac{1}{V}\int d\mathbf{r}\; q_2(\mathbf{r},s)q_2^\dagger(\mathbf{r},s). \quad (3)$$

Here $q_i(\mathbf{r},s)$ and $q_i^\dagger(\mathbf{r},s)$ ($i = 1$ and 2) are the propagators of the two polymers, satisfying the following modified diffusion equations,[54]

$$\frac{\partial q_1(\mathbf{r},s)}{\partial s} = \nabla^2 q_1(\mathbf{r},s) - w(\mathbf{r},s)q_1(\mathbf{r},s), \quad (4)$$

$$-\frac{\partial q_1^\dagger(\mathbf{r},s)}{\partial s} = \nabla^2 q_1^\dagger(\mathbf{r},s) - w(\mathbf{r},s)q_1^\dagger(\mathbf{r},s), \quad (5)$$

$$\frac{\partial q_2(\mathbf{r},s)}{\partial s} = \nabla^2 q_2(\mathbf{r},s) - w(\mathbf{r},s)q_2(\mathbf{r},s), \quad (6)$$

$$-\frac{\partial q_2^\dagger(\mathbf{r},s)}{\partial s} = \nabla^2 q_2^\dagger(\mathbf{r},s) - w(\mathbf{r},s)q_2^\dagger(\mathbf{r},s), \quad (7)$$

where $w(\mathbf{r},s) = w_K(\mathbf{r})$ when $s$ belongs to the K-blocks. In the above expressions, the radius of gyration of a linear polymer with the same length to the copolymer $(A'B)_n$, $R_g = N^{1/2}b/\sqrt{6}$ is chosen as the unit of length. The partial differential equations are integrated with the variable range of $s \in [0,\ \gamma]$ for AB diblock and $s \in [0,\ 1]$ for $(A'B)_n$ star, and with the initial conditions, $q_1(\mathbf{r},0) = q_2(\mathbf{r},1/n) = 1$, $q_1^\dagger(\mathbf{r},\gamma) = 1$, and $q_2^\dagger(\mathbf{r},0) = [q_2(\mathbf{r},0)]^{(n-1)}$. Minimization of the free energy functional with respect to the

View Article Online
DOI: 10.1039/C7CP03718J



density and field functions leads to the standard SCFT equations,[36]

$$w_{\rm A}(\mathbf{r}) = \chi_{\rm AB}N\phi_{\rm B}(\mathbf{r}) + \chi_{\rm AA'}N\phi_{\rm A'}(\mathbf{r}) + \eta(\mathbf{r}), \quad (8)$$

$$w_{\rm A'}(\mathbf{r}) = \chi_{\rm A'B}N\phi_{\rm B}(\mathbf{r}) + \chi_{\rm AA'}N\phi_{\rm A}(\mathbf{r}) + \eta(\mathbf{r}), \quad (9)$$

$$w_{\rm B}(\mathbf{r}) = \chi_{\rm AB}N\phi_{\rm A}(\mathbf{r}) + \chi_{\rm A'B}N\phi_{\rm A'}(\mathbf{r}) + \eta(\mathbf{r}), \quad (10)$$

$$\phi_{\rm A}(\mathbf{r}) = \gamma\int_0^{f_1} ds\, q_1(\mathbf{r},s)q_1^{\dagger}(\mathbf{r},s), \quad (11)$$

$$\phi_{\rm A'}(\mathbf{r}) = z_2 n\int_0^{f_2/n} ds\, q_2(\mathbf{r},s)q_2^{\dagger}(\mathbf{r},s), \quad (12)$$

$$\phi_{\rm B}(\mathbf{r}) = \gamma\int_{f_1}^{1} ds\, q_1(\mathbf{r},s)q_1^{\dagger}(\mathbf{r},s) + z_2 n\int_{f_2/n}^{1/n} ds\, q_2(\mathbf{r},s)q_2^{\dagger}(\mathbf{r},s). \quad (13)$$

We solve the SCFT equations using the pseudospectral method[57,58] and implement the Anderson mixing iteration scheme[59] to accelerate the converging speed. A unit cell method is applied to determine the free energy for each candidate ordered phase, where the box size is optimized to release the stress in the cell. Specifically, a two-dimensional (2D) box is used for the cylindrical phases while a three-dimensional box for the spherical BCC and FCC phases. Periodic boundary condition is imposed on each direction of the cell that is divided into 64 or 128 grids with a grid spacing smaller than $0.1R_g$, and the step size for the chain contour is set up as $\Delta s = 0.005$ or 0.002. Because the average concentration, $\phi_1$, of the AB diblock is conjugated to $z_2$ and $\gamma$, via the relationship $\phi_1 = \gamma Q_1 = 1.0 - z_2 Q_2$, the results from the calculations in the grand canonical ensemble can be readily expressed in terms of the canonical variable $\phi_1$.

## 3 Results and Discussion

For the current binary blend of block copolymers, there are at least seven parameters, including two interaction parameters ($\chi_{\rm AB}N = \chi_{\rm A'B}N$, $\chi_{\rm AA'}N$), two block ratios ($f_1$, $f_2$), the length ratio $\gamma$, the number of arms ($n$) of the star copolymer, and the average composition of the copolymers ($\phi_1$). Obviously, it is a formidable task to blindly search the entire parameter space for the desired phase. Instead it is important to fix certain parameters and explore the restricted parameter space spanned by the rest of the parameters. In our previous study, it has been established that the effect of combinatorial entropy resulting in a tendency for the multiple arms to be distributed in different neighboring domains, thus forming effective bonds between them. This effect becomes significantly important when the arm number $n \geq 4$.[35] Therefore, we consider $n = 5$ in the current study. Furthermore, because our primary goal is to obtain stable square cylindrical phase, we fix $\chi_{AB}N = 50$ and $f_1 = 0.24$ such that the AB diblock forms the hexagonal cylindrical phase.[24] With this set of fixed parameters, we are able to focus on the impact of the three nontrivial parameters, $\chi_{\rm AA'}N$, $f_2$ and $\gamma$, on the self-assembly behavior of the binary blends with varying $\phi_1$.

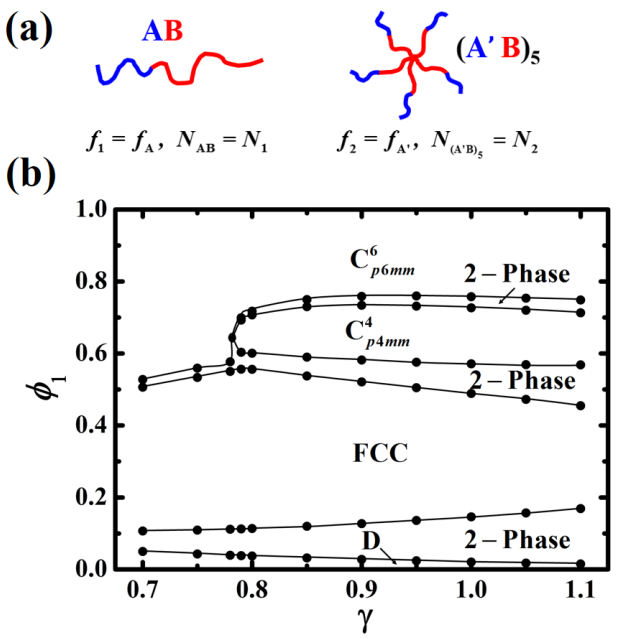


**Fig. 1** (a) Schematic plots for the two polymer molecules in the considered blend. (b) Phase diagram in the $\gamma - \phi_1$ plane for the binary blend of AB diblock and $(\rm A'B)_5$ star copolymers with $\chi_{\rm AB}N = 50$, $f_1 = 0.24$, $f_2 = 0.30$, and $\chi_{\rm AA'}N = -20$, obtained by the SCFT calculations in the grand-canonical ensemble. The solid lines are guide for the eyes, and the coexistence region delimiting two neighboring phases is labeled by "2-phase".

### 3.1 Effect of the Length Ratio $\gamma$

The key principle to obtain the tetragonal cylinders instead of the hexagonal cylinders is to regulate bridging blocks via the local segregation of the two block copolymers inside the matrix. This regulation could be achieved by tailoring the controlling parameters so as to localize the highly stretched $(\rm A'B)_n$ star copolymers in the bonding area between two neighboring A-domains while distribute the long AB diblocks into the central area surrounding the neighboring A-domains. In other words, the junction point of the star copolymer is assumed to be located at the center of the connection line of two neighboring domains in the tetragonal phase while the diblock copolymer is stretched from the center of each domain to the center of each square unit. Accordingly the end-to-end distance of each arm of the star copolymer is nearly half the side length of the square unit, and that of the diblock copolymer is $\sqrt{2}$ of half the side length. Based on this argument, we could roughly estimate that $N_1^{1/2} > \sqrt{2}(N_2/n)^{1/2}$ when considering the nonuniform distribution, i.e. $\gamma = N_1/N_2 > 2/n = 0.4$. A larger $\gamma$ gives rise to a larger difference of lengths between the diblock and each arm of the star, thus leading to a higher degree of local segregation between the two copolymers that ultimately transforms into the macroscopic separation. On the other hand, the macrophase separation can be suppressed by a negative $\chi_{\rm AA'}N$.

We first examine the effect of $\gamma$ on the self-assembly of the binary blends with variable composition $\phi_1$ for fixed values of $\chi_{\rm AA'}N = -20$ and $f_2 = 0.3$. The phase diagram at the $\gamma$-$\phi_1$ plane is constructed by considering four candidate ordered phases, in-

View Article Online
DOI: 10.1039/C7CP03718J



cluding hexagonal cylindrical phase ($C^6_{p6mm}$), square cylindrical phase ($C^4_{p4mm}$), face-centered-cubic (FCC) spherical phase and body-centered-cubic (BCC) spherical phase (Figure 1). The typical free-energy comparison together with the four morphological plots is given in Figure 2. Additionally, the absolute values of free energy of each phase are listed in Table 1. Note that a set of standard skills have been established to guarantee the accuracy of the free energy of each ordered phase for the pseudo-spectral method of SCFT, including converging the solution efficiently, optimizing the dimension of the unit cell and fining the grid spacing. In our previous work,[60,61] It has been demonstrated that the pseudo-spectral method is able to determine the free energy difference as tiny as $10^{-7} \sim 10^{-5} k_B T$ per chain. Therefore, the results of the small free-energy difference between the FCC and BCC phases in Figure 2 are reliable.In the phase diagram of Figure 1, $\phi_1 = 0$ corresponds the pure star copolymers that do not phase separate forming a disordered phase with $\chi_{A'B}N = 50$, and our calculation predicts that the order-disorder transition (ODT) of $(A'B)_5$ is $(\chi_{A'B}N)_{ODT} \approx 58.46$ for $f_2 = 0.3$. Note that $(\chi_{A'B}N)_{ODT}/5 \approx 11.7$ is significantly lower than the corresponding ODT of AB diblock, $(\chi_{AB}N)_{ODT} \approx 14.0$, at $f_A = 0.3$.[24,62] This shift of ODT originating from the loss of translational entropy due to the joint of multiple diblocks is commonly observed in this type of multi-arm star copolymers of which $n = 2$ leads to the special sample of ABA triblock copolymer.[23,24]

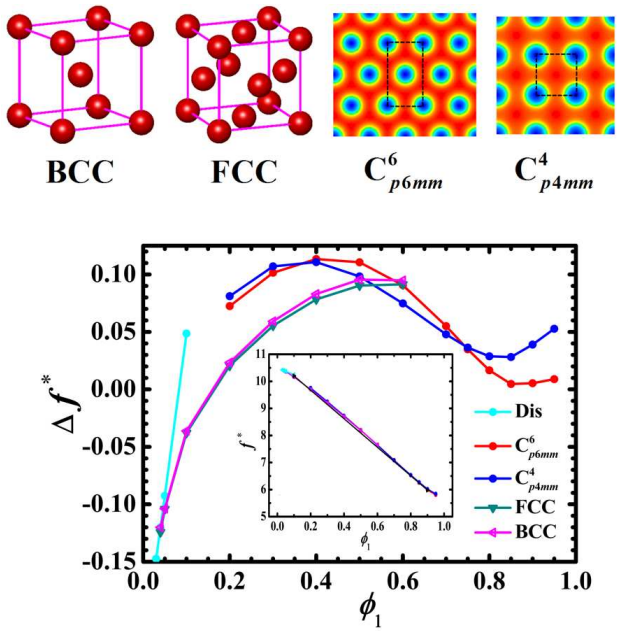


**Fig. 2** Density plots of four candidate morphologies as well as their free energy comparison as a function of $\phi_1$ in the canonical ensemble for $\gamma = 1.0$ and the same set of other parameters as those of Figure 1. For clarity, we shift the dimensionless free energy, $f^* = NF/V\rho_0 k_B T$, to be $\Delta f^* = N\Delta F/V\rho_0 k_B T = NF/V\rho_0 k_B T - g(\phi_1)$ where $g(\phi_1) = -5.275(\phi_1 - 0.1) + 10.2$ represents an oblique line. The inset shows the free energy $f^*$ together with the oblique line $g(\phi_1)$ displayed in black color. The stable phase sequence is from disorder, to FCC, $C^4_{p4mm}$, and $C^6_{p6mm}$ as $\phi_1$ increases.

Because the added diblocks are with a length of $\gamma N$ much longer than each arm of the star in the range of $0.7 \leq \gamma \leq 1.1$, the segregation degree of the blend increases as the diblocks are added, resulting in a phase transitions from disorder, to sphere, and then to hexagonal cylinder that is the stable phase of the pure diblock with a fixed volume fraction of $f_1 = 0.24$. It has been established that many AB-type block copolymers share a generic phase transition sequence from the disordered phase to the hexagonal close-packing (HCP) spheres, the BCC spheres, the $C^6_{p6mm}$ cylinders, gyroids, and lamellae.[24] For the HCP phase, there are two types of stacking, $abab\cdots$ and $abcabc\cdots$ (or FCC), which have slightly different free energy.[63] Here we simply consider the FCC phase instead of the HCP phase with the $abab\cdots$ stacking, which would not change the phase boundaries noticeably because of their tiny free-energy difference. Interestingly, FCC occupies a large window of stability while BCC does not appear in the phase diagram shown in Figure 1. This observation is in marked contrast to the phase diagram of many AB-type block copolymers that usually possesses a dominant BCC region over FCC.[24] We will discuss the underlying mechanism later.

Surprisingly, the square cylindrical phase, $C^4_{p4mm}$, becomes stable after FCC as $\phi_1$ is increased further, and more importantly, it possesses a considerable stability region between the FCC and $C^6_{p6mm}$ phases. As expected, two neighboring phases is separated by their coexistence region. Obviously, these coexistence regions becomes wider as $\gamma$ increases, i.e. that the length difference of the diblock and the diblock arm of the star increases. To accommodate two types of blocks with a larger difference of length into the same domains causes a higher entropy penalty. Another interesting feature is that the $C^4_{p4mm}$ phase starts to become stable when $\gamma \gtrsim 0.79$ and the width of its stable region only varies gently. This indicates that there is a critical value of $\gamma$ for stabilizing the $C^4_{p4mm}$ phase. For $\gamma \gtrsim 0.79$, a delicate balance between the local segregation and the macrophase separation is reached under the interplay between the incompatibility induced by the mismatched chain length and the attractive interaction of A and A′ blocks, which leads to the formation of stable $C^4_{p4mm}$ phase in the region of $0.6 \lesssim \phi_1 \lesssim 0.7$.

### 3.2 Effect of Attractive Interaction $\chi_{AA'}N$

As mentioned above, the attractive interaction $\chi_{AA'}N$ plays a key role in suppressing the macroscopic phase separation of the two different block copolymers. From practical point of view, a weaker $\chi_{AA'}N$ is easier to be achieved via non-covalent bonding interactions. To gain quantitative information about the effect of $\chi_{AA'}N$, we construct a phase diagram in the $(-\chi_{AA'}N) - \phi_1$ plane for the case of $\gamma = 1$ and $f_2 = 0.3$ (Figure 3). In this phase diagram, the most important feature is that the phase region of the desired $C^4_{p4mm}$ tapers off until vanishing at $(-\chi_{AA'}N) \approx 11.7$ as $(-\chi_{AA'}N)$ decreases, which is mainly due to the invasion of the expanding coexistence regions.

### 3.3 Effect of the Volume Fraction $f_2$

So far we only consider the case of $f_2 = 0.3$, where the length of the A-block in each arm of the star $0.06N$ is much shorter than

View Article Online
DOI: 10.1039/C7CP03718J



**Table 1** List of the absolute values of free energy of each phase shown in the inset of Figure 2.

| Phase/$\phi_1$ | $C^6_{p6mm}$ | $C^4_{p4mm}$ | FCC | BCC | Dis |
|---|---|---|---|---|---|
| 0.03 | – | – | – | – | 10.421934 |
| 0.04 | – | – | 10.392182 | 10.392209 | 10.396416 |
| 0.05 | – | – | 10.359603 | 10.359882 | 10.371150 |
| 0.10 | – | – | 10.162094 | 10.163776 | 10.248600 |
| 0.20 | 9.744986 | 9.753640 | 9.693131 | 9.695905 | – |
| 0.30 | 9.246483 | 9.252051 | 9.200427 | 9.204176 | – |
| 0.40 | 8.730912 | 8.728271 | 8.695740 | 8.700436 | – |
| 0.50 | 8.200807 | 8.188347 | 8.180299 | 8.185459 | – |
| 0.60 | 7.653118 | 7.637288 | 7.653889 | 7.657375 | – |
| 0.70 | 7.090095 | 7.082851 | – | – | – |
| 0.80 | 6.524101 | 6.536341 | – | – | – |
| 0.90 | 5.985347 | 6.018957 | – | – | – |
| 0.95 | 5.801158 | 5.843375 | – | – | – |

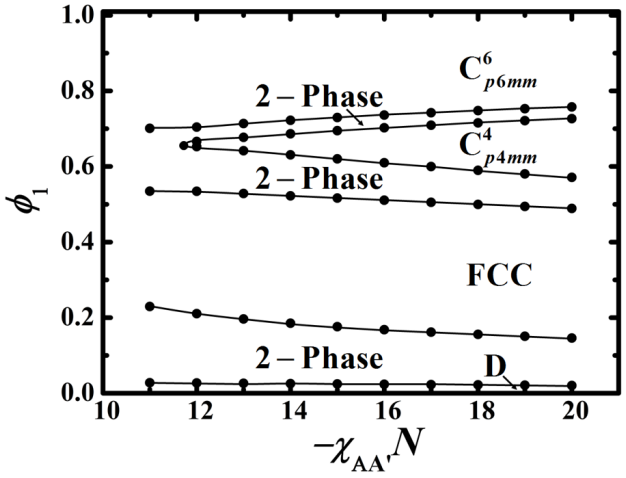


**Fig. 3** Phase diagram in the $(-\chi_{AA'}N)-\phi_1$ plane for the binary blend with fixed $\gamma=1.0$ and the same $\chi_{AB}N$, $f_1$ and $f_2$ as those of Figure 1.

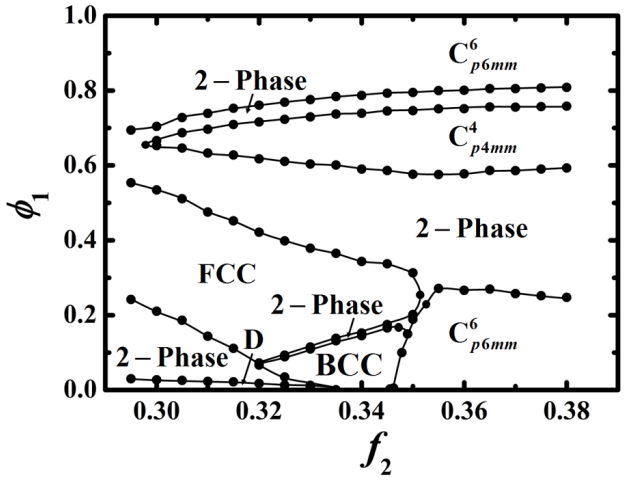


**Fig. 4** Phase diagram in the $f_2$-$\phi_1$ plane for the binary blend with fixed $\gamma=1.0$ and $\chi_{AA'}N=-12$.

that of the diblock $\gamma f_1 N$ when $\gamma \gtrsim 0.79$. For such short A-blocks with $f_2=0.3$, the bulk phase of the star copolymers is disordered. Intuitively, the bulk phase of the star copolymers should influence the self-assembly behavior of the binary blends. In order to examine this influence, the phase diagram in the $f_2-\phi_1$ plane for the case of $\gamma=1.0$ and $(-\chi_{AA'}N)=12$ is constructed (Figure 4). Moreover, the value of $f_2$ is restricted in the range $0.295 \le f_2 \le 0.38$, in which the bulk phase of the star copolymers changes from the disordered phases to spheres and cylinders. It is noted that the spherical phase of the star copolymers is BCC but not FCC in this region of the phase diagram.[24]

Obviously, the phase transition sequences of the blends depend on the value of $f_2$. One interesting sequence, from BCC to FCC, $C^4_{p4mm}$, and $C^6_{p6mm}$, is found for $f_2 \sim 0.34$. Along this path, the coexistence region of the BCC and FCC phases is very narrow, which provides opportunities for experiments to explore the phase transition from BCC to FCC. Regardless of the bulk phase of the star copolymers, a stable region of the $C^4_{p4mm}$ phase is always present except for $f_2 \lesssim 0.297$. As $f_2$ is increased, the phase region of $C^4_{p4mm}$ becomes wider, reaching a maximum at $f_2 \approx 0.355$, and then tapers off slowly. It is noted that the phase region of $C^4_{p4mm}$ would be terminated by the presence of the gyroid phase at the direction of increasing $f_2$.

### 3.4 Analysis of the Transition Mechanism

The SCFT provides not only accurate free energy for different ordered phases, but also the distribution of the polymer chains. The distribution of the different segments of the polymers enables us to probe into the formation mechanism of various ordered phases. Specifically, we will examine the transition mechanism between the $C^6_{p6mm}$ and $C^4_{p4mm}$ phases, as well as that between the BCC and FCC phases. In a previous study, it has been shown that the change of CN of the cylindrical phases could be induced by adjustable effective bond.[35] In what follows we will provide detailed evidences for the construction of the effective bond as well as its length adjustability.

As discussed above, an effective bond is formed by the star copolymers that distribute their multiple arms into different neighboring domains. In order to examine this effect, in Figure 5 we plot the distribution of the junction points of the star copolymers along a typical phase path ($f_2=0.36$ in Figure 4), The junction distribution is defined by, $\phi_{\text{junction}}(\mathbf{r})=(1-\phi_1)q_2(\mathbf{r},\ 0.2)q_2^{\dagger}(\mathbf{r},\ 0.2)/Q_2$, which was obtained in the canonical ensemble with various values of $\phi_1=0.1,\ 0.2,\ \cdots,\ 0.9$. For

View Article Online
DOI: 10.1039/C7CP03718J



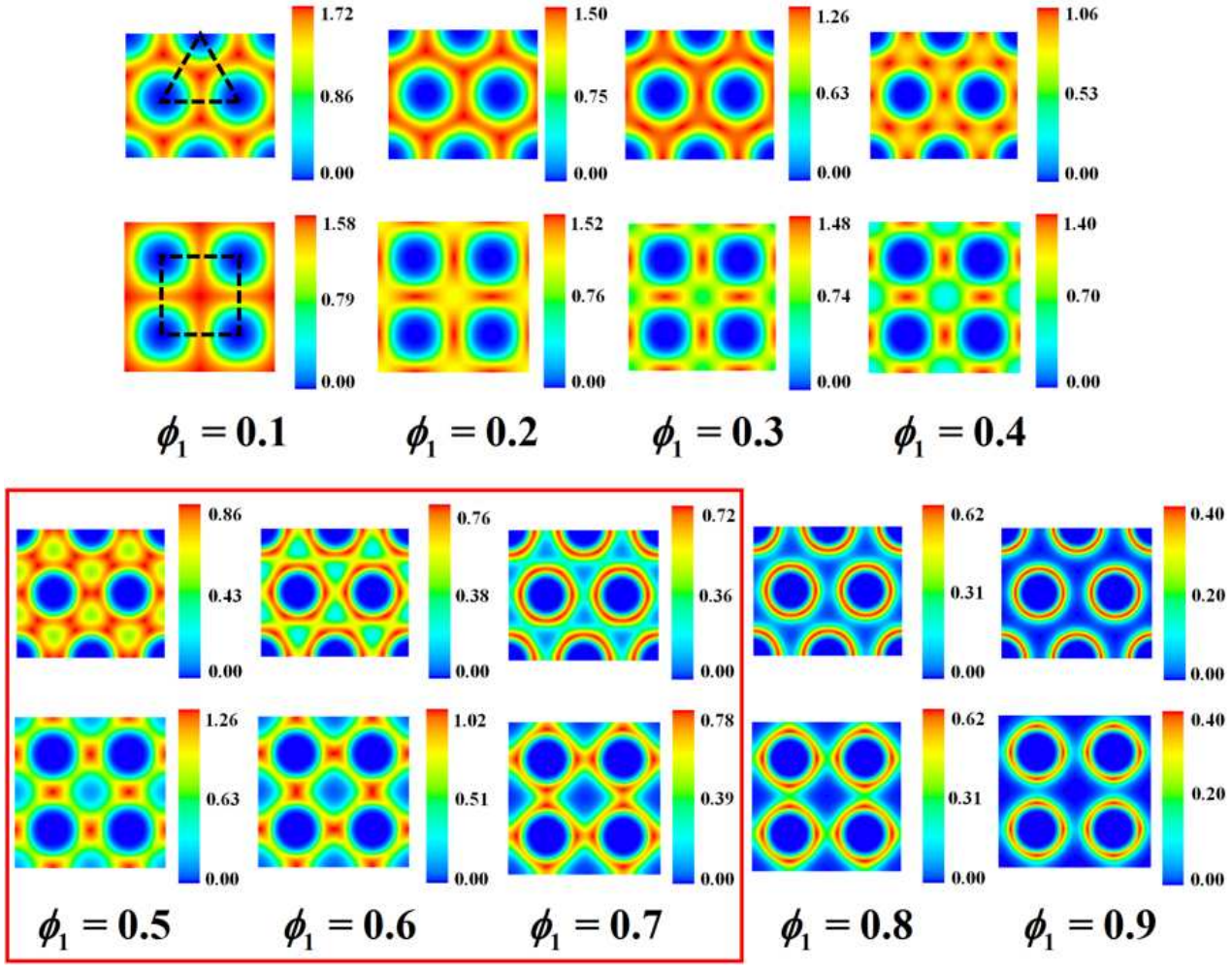


**Fig. 5** Distribution of the junction point of $(\mathrm{A'B})_5$ star copolymers in the $\mathrm{C}^4_{p4mm}$ and $\mathrm{C}^6_{p6mm}$ cylindrical phases, $\phi_{\mathrm{junction}}(\mathbf{r}) = (1-\phi_1)q_2(\mathbf{r},\ 0.2)q_2^{\dagger}(\mathbf{r},\ 0.2)/Q_2$, determined by the SCFT calculations in the canonical ensemble for various contents of AB diblock copolymers along the phase path $f_2 = 0.36$ in the phase diagram of Figure 4. Note that each distribution has its own color spectrum. For high content of the star copolymers, i.e. with small $\phi_1$, the junction point is more likely to be located at the center of the triangular/square area of the hexagonal/square phase indicated by the dashed lines in the plots of $\phi_1 = 0.1$. For $\phi_1 = 0.5$, 0.6, and 0.7, $\mathrm{C}^4_{p4mm}$ has lower free energy than $\mathrm{C}^6_{p6mm}$ in the canonical ensemble calculations, highlighted by the red rectangular box.

View Article Online
DOI: 10.1039/C7CP03718J



$\phi_1 = 0.1$, the majority component of the blends is the $(A'B)_5$ star copolymer. In either hexagonal or square cylindrical morphology, the junction points are distributed almost uniformly around each domain, with very weak peaks at the center of the triangle or square constructed by bonds connecting nearest neighbor domains. The presence of this peak provides a direct evidence illustrating the effect of combinatorial entropy, because localizing the junction of the star copolymers at the center of the triangular or square cell would result in the largest probability of the star copolymers partitioning their multiple arms into the largest number of domains. Although the square phase benefits from the combinatorial entropy, it has a higher energy penalty induced by the highly nonuniform stretching of the majority blocks and thus is less stable than the hexagonal phase.

The addition of the AB diblock copolymers to the blends, or increasing $\phi_1$, leads to the swelling of the cylindrical morphologies. Furthermore, the longer B-blocks of the diblock copolymers tend to fill the highly-stretched region corresponding to the center of the triangular or square cells, whereas the shorter B-blocks of the star copolymers are preferentially located at the areas between two nearest domains or the *bonding* areas. This nonuniform distribution of the polymeric segments results in the formation of effective bond connecting two nearest neighboring domains. This effect is much more pronounced in the square phase than in the hexagonal phase. On the other hand, this redistribution of the star copolymers is accompanied by a loss of the combinatorial entropy because the number of domains accessible to one star copolymer is reduced from 3 of the hexagonal phase (or 4 of the square phase) to 2. The star copolymers located in the bonding area become more stretched as $\phi_1$ is increased. In contrast to our previous work in which the length of effective bonds is adjusted directly by varying the length of the bridging blocks,[35] the length of the bridging blocks is unchanged while the domains as well as their spacing is enlarged by swelling longer diblock copolymers into the star copolymers with much shorter diblock arms. Despite this difference in details, the two mechanisms have an equivalent effect on regulating the domain arrangement.

When the star copolymers are highly stretched, there at least exists one pair of arms whose ends are separately located in two different neighboring domains. Therefore, the stretching degree of the star copolymer can be measured by the domain spacing $d$ relative to the ideal end-to-end distance of a polymer chain with a twice length of the diblock arm, $d_e = \sqrt{12/5}R_g \approx 1.55R_g$. The calculated $d/d_e$ as a function of $\phi_1$ for the two competing cylindrical phases is presented in Figure 6. Obviously, the stretching of the star copolymers is stronger in the hexagonal phase than that in the square phase. This difference is amplified for $\phi_1 > 0.5$. The underlying mechanism is similar to that in the binary crystalline phases.[64] One mechanism to release the high stretching is to disrupt the effective bonds by localizing all arms of each star copolymer into a single domain, which results in a large loss of the combinatorial entropy. Compared with the hexagonal phase, the disruption of the effective bond in the square phase is delayed due to its smaller domain size and spacing (Figure 5). As a result, the hexagonal phase transforms into the square phase at $\phi_1 \approx 0.42$ in the calculations of canonical ensemble, where the coexistence

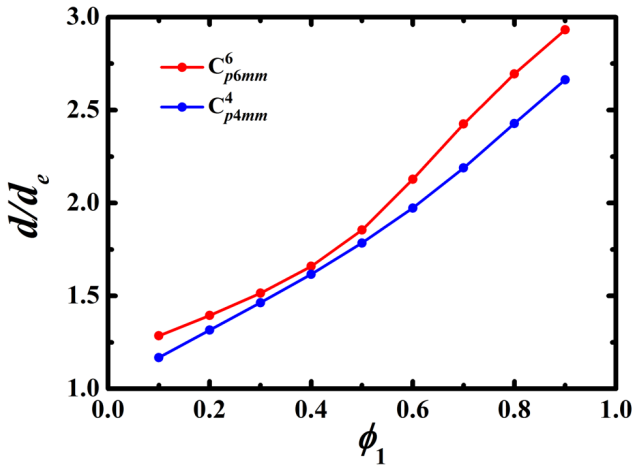


**Fig. 6** Cylinder-to-cylinder distance $d$ of the $C^4_{p4mm}$ and $C^6_{p6mm}$ cylindrical phases, relative to the ideal end-to-end distance $d_e = \sqrt{12/5}R_g$ of a linear polymer with a twice length of the diblock arm of the star copolymer, along the phase path $f_2 = 0.36$ in Figure 4.

region of two neighboring phases that usually exists in the blending system is not included. In other words, this transition is a consequence of the competition between the combinatorial entropy and other free-energy contributions. Of course, at very large $\phi_1$, the effective bond in the square cylinders is also too stretched to be maintained (Figure 5), i.e. $d/d_e \approx 2.43$ for $\phi_1 = 0.8$. The disruption of the effective bonds makes the square phase to lose its advantage in the combinatorial entropy and therefore to transform back into the hexagonal phase.

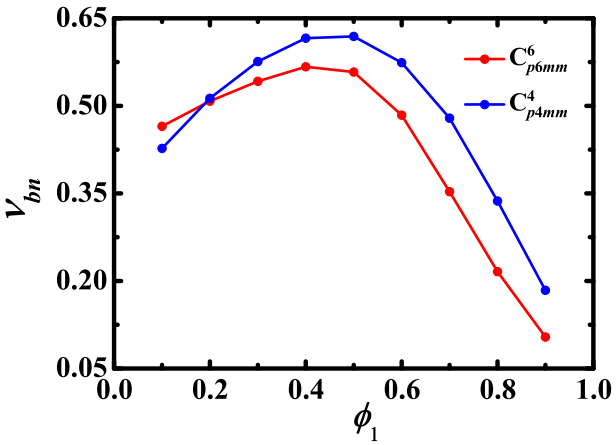


**Fig. 7** Comparison of the ratio of the bridging configurations connecting a pair of neighboring domains between the hexagonal and square cylindrical phases for the same system in Figure 5.

As discussed above, the bridges are mainly formed in the form of the bridging configurations connecting a pair of neighboring domains, of which at least one arm of the star copolymer is located in each of the pair of domains. To more quantitatively demonstrate the difference of variation of the bridges between the hexagonal and square phases as $\phi_1$, we calculate the ratio of the bridging configurations connecting a pair of neighboring do-

View Article Online
DOI: 10.1039/C7CP03718J



mains, $v_{bn}$, according to the algorithm proposed in Ref. [52] (Figure 7). The comparison indicates that the value of $v_{bn}$ of $C^4_{p4mm}$ becomes higher than that of $C^6_{p6mm}$ when $\phi_1 \geq 0.2$, and the difference increases in the range of $0.2 \leq \phi_1 < 0.7$. Moreover, the value $v_{bn}$ of $C^4_{p4mm}$ increases to be higher than 50% at $\phi_1 = 0.2$ and then decreases after passing the maximal point at around $\phi_1 = 0.5$, in particular, becoming lower than 50% when $\phi_1 \geq 0.7$. This observation further rationalizes the transition from the hexagonal phase to the square phase, and then back to the hexagonal phase.

## 4 Conclusions

In summary, the self-assembly behaviours of binary blends composed of AB diblock and $(A'B)_5$ star copolymers are studied using the polymeric self-consistent field theory. A negative interaction parameter $\chi_{AA'}N$ is introduced to mimic the non-covalent attractive interactions, such as the hydrogen bond, between the two A-type blocks. The study focuses on the occurrence and stability of the square cylindrical, or $C^4_{p4mm}$, phase. For simplicity, the volume fraction of the diblock copolymers, $f_1 = 0.24$, as well as the interaction parameters $\chi_{AB}N = \chi_{A'B}N = 50$ are kept as constant in the current study, while the length ratio of the two copolymers, $\gamma$, the composition of the star copolymers, $f_2$, and the $\chi_{AA'}N$ are chosen as controlling parameters. Two-dimensional phase diagrams with respect to the volume fraction of the AB diblocks and each of the controlling parameters are constructed via the SCFT calculations in the grand-canonical ensemble. Considerable stability windows for the square phase are predicted to occur in these phase diagrams. Interestingly, there is a general phase transition sequence, from the bulk disordered or BCC phase of the star copolymers to FCC, $C^4_{p4mm}$, and finally to the bulk $C^6_{p6mm}$ phase of the AB diblocks, or from the bulk $C^6_{p6mm}$ phase of the star copolymers to $C^4_{p4mm}$, and then to $C^6_{p6mm}$ phase. Of course, two neighboring phases are separated by their coexistence regions. Importantly, the stability region of the desired $C^4_{p4mm}$ phase could be regulated by the magnitude of $\chi_{AA'}N$ and it could become considerably wide. In particular, a notable phase region of $C^4_{p4mm}$ is predicted for a fixed weak $\chi_{AA'}N = -12$ relative to the magnitude of $\chi_{AB}N = 50$ by tailoring the compositions and length ratio of the two copolymers. This formulation of the block copolymer blends could be readily accessible by experiments.[46]

The transition mechanisms of the various phase transitions observed from the SCFT calculations are rationalized in the context of the construction and degeneration of the effective bonds bridging neighboring cylindrical domains. Effective bonds connecting two polymeric domains are formed by the star copolymers due to the effect of combinatorial entropy. When the longer AB diblocks are added into the star copolymers, the domains are swollen leading to larger domain size and domain spacing. As a consequence, the star copolymers become more and more stretched. Local segregation of the diblock and star copolymers in the form of bonding areas and filling areas could lead to the release of this stretching energy, albeit at a cost of the combinatorial entropy of the star copolymers. When more AB diblock copolymers are added, the star copolymers in the hexagonal cylinders would be too stretched to bridge two neighboring domains, resulting in a disruption of the effective bonds. One effective way for the self-assembly system to delay this bond disruption is to form a new array of less-coordinated cylinders, i.e. the square phase of $C^4_{p4mm}$ whose smaller domain size and spacing is helpful to reduce the extra stretching of the effective bonds. When most of the bridge configurations are unavoidably disrupted in the $C^4_{p4mm}$ phase due to the extreme swelling of the AB diblocks, the $C^4_{p4mm}$ phase loses its advantage in the combinatorial entropy and therefore transforms back into $C^6_{p6mm}$. Finally we would like to emphasize that the current work demonstrated a mechanism of regulating the cylindrical arrangement between the hexagonal and square lattices via the local segregation of two different copolymers. At the same time, it provides an alternative route to engineering the square cylindrical phase.

## 5 Acknowledgements

This work was supported by National Natural Science Foundation of China (Grants Nos 21574026, 21322407, and 21320102005). A.-C. Shi acknowledges the support from the Natural Science and Engineering Research Council (NSERC) of Canada.

## References

1 F. S. Bates and G. H. Fredrickson, *Physics Today*, 1999, **52**, 32–38.
2 C. T. Black, K. W. Guarini, K. R. Milkove, S. M. Baker, T. P. Russell and M. T. Tuominen, *Appl. Phys. Lett.*, 2001, **79**, 409–411.
3 W. A. Lopes and H. M. Jaeger, *Nature*, 2001, **414**, 735–738.
4 V. Abetz and P. F. W. Simon, *Adv. Polym. Sci.*, 2005, **189**, 125–212.
5 R. A. Segalman, *Mater. Sci. Eng. R*, 2005, **48**, 191–226.
6 E. J. W. Crossland, M. Nedelcu, C. Ducati, S. Ludwigs, M. A. Hillmyer, U. Steiner and H. J. Snaith, *Nano Lett.*, 2009, **9**, 2813–2819.
7 T. Hashimoto, K. Tsutsumi and Y. Funaki, *Langmuir*, 1997, **13**, 6869–6872.
8 S. O. Kim, H. H. Solak, M. P. Stoykovich, N. J. Ferrier, J. J. de Pablo and P. F. Nealey, *Nature*, 2003, **424**, 411–414.
9 R. Ruiz, H. Kang, F. A. Detcheverry, E. Dobisz, D. S. Kercher, T. R. Albrecht, J. J. de Pablo and P. F. Nealey, *Science*, 2008, **321**, 936–939.
10 R. A. Griffiths, A. Williams, C. Oakland, J. Roberts, A. Vijayaraghavan and T. Thomson, *J. Phys. D: Appl. Phys.*, 2013, **46**, 503001.
11 T. Thurn-Albrecht, J. Schotter, G. A. Kastle, N. Emley, T. Shibauchi, L. Krusin-Elbaum, K. Guarini, C. T. Black, M. T. Tuominen and T. P. Russell, *Science*, 2000, **290**, 2126–2129.
12 X. M. Yang, S. G. Xiao, C. Liu, K. Pelhos and K. Minor, *J. Vac. Sci. Technol. B*, 2004, **22**, 3331–3334.
13 M. P. Stoykovich, M. Müller, S. O. Kim, H. H. Solak, E. W. Edwards, J. J. de Pablo and P. F. Nealey, *Science*, 2005, **308**, 1442–1446.
14 M. P. Stoykovich, H. Kang, K. C. Daoulas, G. L. Liu, C.-C. Liu, J. J. de Pablo, M. Müller and P. F. Nealey, *ACS Nano*, 2007, **1**, 168–175.

View Article Online
DOI: 10.1039/C7CP03718J



15 L. Zhang, L. Wang and J. Lin, *ACS Macro Lett.*, 2014, **3**, 712–716.
16 J.-B. Chang, H. K. Choi, A. F. Hannon, A. Alexander-Katz, C. A. Ross and K. K. Berggren, *Nat. Commun.*, 2014, **5**, 3305.
17 M. Park, C. Harrison, P. M. Chaikin, R. A. Register and D. H. Adamson, *Science*, 1997, **276**, 1401–1404.
18 S. B. Darling, *Prog. Polym. Sci.*, 2007, **32**, 1152–1204.
19 I. W. Hamley, *Prog. Polym. Sci.*, 2009, **34**, 1161–1210.
20 W. H. Li and M. Müller, *Prog. Polym. Sci.*, 2016, **54-55**, 47–75.
21 C. G. Hardy and C. B. Tang, *J. Poly. Sci., Part B: Polym. Phys.*, 2013, **51**, 2–15.
22 M. W. Matsen and M. Schick, *Phys. Rev. Lett.*, 1994, **72**, 2660–2663.
23 M. W. Matsen and R. B. Thompson, *J. Chem. Phys.*, 1999, **111**, 7139–7146.
24 M. W. Matsen, *Macromolecules*, 2012, **45**, 2161–2165.
25 S.-M. Hur, C. J. Garcia-Cervera, E. J. Kramer and G. H. Fredrickson, *Macromolecules*, 2009, **42**, 5861–5872.
26 J. Xu, T. P. Russell, B. M. Ocko and A. Checco, *Soft Matter*, 2011, **7**, 3915–3919.
27 W. B. Lee, R. Elliott, R. Mezzenga and G. H. Fredrickson, *Macromolecules*, 2009, **42**, 849–859.
28 Y. Mogi, H. Kotsuji, Y. Kaneko, K. Mori, Y. Matsushita and I. Noda, *Macromolecules*, 1992, **25**, 5408–5411.
29 Y. Mogi, M. Nomura, H. Kotsuji, K. Ohnishi, Y. Matsushita and I. Noda, *Macromolecules*, 1994, **27**, 6755–6760.
30 M. W. Matsen, *J. Chem. Phys.*, 1998, **108**, 785–796.
31 J. G. Son, J. Gwyther, J.-B. Chang, K. K. Berggren, I. Manners and C. A. Ross, *Nano Lett.*, 2011, **11**, 2849–2855.
32 F. S. Bates, M. A. Hillmyer, T. P. Lodge, C. M. Bates, K. T. Delaney and G. H. Fredrickson, *Science*, 2012, **336**, 434–440.
33 R. Martin-Rapun, M. Marcos, A. Omenat, J. Barberá, P. Romero and J. L. Serrano, *J. Am. Chem. Soc.*, 2005, **127**, 7397–7403.
34 N. Canilho, E. Kase1mi, A. D. Schlu1ter and R. Mezzenga, *Macromolecules*, 2007, **40**, 2822–2830.
35 Y. Gao, H. L. Deng, W. H. Li, F. Qiu and A. C. Shi, *Phys. Rev. Lett.*, 2016, **116**, 068304.
36 M. W. Matsen, *Macromolecules*, 1995, **28**, 5765–5773.
37 M. P. Stoykovich, E. W. Edwards, H. H. Solak and P. F. Nealey, *Phys. Rev. Lett.*, 2006, **97**, 147802.
38 Y.-C. Wang, M. I. Kim, S. Akasaka, K. Saijo, H. Hasegawa, T. Hikima and M. Takenaka, *Macromolecules*, 2016, **49**, 2257–2261.
39 V. Abetz and T. Goldacker, *Macromol. Rapid Commun.*, 2000, **21**, 16–24.
40 M. J. Liu, B. K. Xia, W. H. Li, F. Qiu and A.-C. Shi, *Macromolecules*, 2015, **48**, 3386–3394.
41 Y. Asai, K. Yamada, M. Yamada, A. Takano and Y. Matsushita, *ACS Macro Lett.*, 2014, **3**, 166–169.
42 M. J. Liu, Y. C. Qiang, W. H. Li, F. Qiu and A.-C. Shi, *ACS Macro Lett.*, 2016, **5**, 1167–1171.
43 A. Dehghan and A.-C. Shi, *Macromolecules*, 2013, **46**, 5796–5805.
44 K. Dobrosielska, S. Wakao, A. Takano and Y. Matsushita, *Macromolecules*, 2008, **41**, 7695–7698.
45 S.-C. Chen, S.-W. Kuo, U.-S. Jeng, C.-J. Su and F.-C. Chang, *Macromolecules*, 2010, **43**, 1083–1092.
46 C. B. Tang, E. M. Lennon, G. H. Fredrickson, E. J. Kramer and C. J. Hawker, *Science*, 2008, **322**, 429–432.
47 J. Kwak, S. H. Han, H. C. Moon and J. K. Kim, *Macromolecules*, 2015, **48**, 6347–6352.
48 D. B. Alward, D. J. Kinning and E. L. Thomas, *Macromolecules*, 1986, **19**, 215–224.
49 X. C. Pang, L. Zhao, M. Akinc, J. K. Kim and Z. Q. Lin, *Macromolecules*, 2011, **44**, 3746–3752.
50 A. B. Burns and R. A. Register, *Macromolecules*, 2016, **49**, 9521–9530.
51 Y. C. Xu, W. H. Li, F. Qiu and Z. Q. Lin, *Nanoscale*, 2014, **6**, 6844–6852.
52 R. K. W. Spencer and M. W. Matsen, *Macromolecules*, 2017, **50**, 1681–1687.
53 A. C. Shi, *Developments in Block Copolymer Science and Technology*, John Wiley & Sons, Ltd., New York, 2004.
54 G. H. Fredrickson, *The Equilibrium Theory of Inhomogeneous Polymers*, Oxford University Press, New York, 2006.
55 M. W. Matsen, *Phys. Rev. Lett.*, 2007, **99**, 148304.
56 V. Pryamitsyn, S. H. Han, J. K. Kim and V. Ganesan, *Macromolecules*, 2012, **45**, 8729–8742.
57 K. Ø. Rasmussen and G. Kalosakas, *J. Polym. Sci., Part B: Polym. Phys.*, 2002, **40**, 1777–1783.
58 G. Tzeremes, K. Ø. Rasmussen, T. Lookman and A. Saxena, *Phys. Rev. E*, 2002, **65**, 041806.
59 R. B. Thompson, K. Ø. Rasmussen, T. Lookman and A. Saxena, *J. Chem. Phys.*, 2004, **120**, 31–34.
60 Y. C. Xu, W. H. Li, F. Qiu, Y. L. Yang and A. C. Shi, *J. Phys. Chem. B*, 2009, **113**, 11153–11159.
61 W. H. Li, M. J. Liu, F. Qiu and A. C. Shi, *J. Phys. Chem. B*, 2013, **117**, 5280–5288.
62 E. W. Cochran, C. J. Garcia-Cervera and G. H. Fredrickson, *Macromolecules*, 2006, **39**, 2449–2451.
63 M. W. Matsen, *Eur. Phys. J. E*, 2009, **30**, 361–369.
64 N. Xie, M. J. Liu, H. L. Deng, W. H. Li, F. Qiu and A.-C. Shi, *J. Am. Chem. Soc.*, 2014, **136**, 2974–2977.

View Article Online
DOI: 10.1039/C7CP03718J



For Table of Contents Use Only